Journal of Controlled Release 349 (2022) 206–212

Contents lists available at ScienceDirect

Journal of Controlled Release

journal homepage: www.elsevier.com/locate/jconrel

Combining lipid based drug delivery and amorphous solid dispersions for improved oral drug absorption of a poorly water-soluble drug

Georgia-Ioanna Nora [a,1], Ramakrishnan Venkatasubramanian [a,1], Sophie Strindberg [a], Scheyla Daniela Siqueira-Jørgensen [a], Livia Pagano [a], Francis S. Romanski [c,d], Nitin K. Swarnakar [c,d], Thomas Rades [a,*], Anette Müllertz [a,b]

[a] Department of Pharmacy, University of Copenhagen, Universitetsparken 4, Copenhagen 2100, Denmark
[b] Bioneer: FARMA, Department of Pharmacy, University of Copenhagen, Universitetsparken 4, Copenhagen 2100, Denmark
[c] BASF Corporation, 500 White Plains Rd., Tarrytown, NY 10591, United States of America
[d] BASF Corporation, Pharma Solutions, 500 White Plains Road, 10591 Tarrytown, United States

ARTICLE INFO

Keywords:
Self-nanoemusifying drug delivery systems (SNEDDS)
Supersaturated SNEDDS (superSNEDDS)
Amorphous solid dispersion (ASD)
Supersaturation
In vitro lipolysis
Pharmacokinetic studies

ABSTRACT

Two widely applied enabling drug delivery approaches, self-nanoemulsifying drug delivery systems (SNEDDS) and amorphous solid dispersions (ASD), were combined, with the aim of enhancing physical stability, solubilization and absorption of the model drug ritonavir. Ritonavir was loaded at a concentration above its saturation solubility (S_{eq}) in the SNEDDS (superSNEDDS, 250% of S_{eq}). An ASD of ritonavir with polyvinylpyrrolidone-vinyl acetate copolymers (Kollidon® VA64) was prepared by ball milling. Relevant control formulations, which include conventional SNEDDS (90% of S_{eq}), superSNEDDS with a physical mix of Kollidon® VA64 and ritonavir (superSNEDDS+PM) and an aqueous suspension of ritonavir were used. A pharmacokinetic (PK) study in rats was performed to assess the relative bioavailability of ritonavir after oral administration. This was followed by evaluating the formulations in a novel two-step *in vitro* lipolysis model simulating rat gastric and intestinal conditions. The addition of a ritonavir containing ASD to superSNEDDS increased the degree of supersaturation from 250% to 275% S_{eq} in the superSNEDDS and the physical stability (absence of drug recrystallization) of the system from 48 h to 1 month under ambient conditions. The PK study in rats displayed significantly higher C_{max} and $AUC_{0\text{-}7h}$ (3-fold increase) and faster T_{max} for superSNEDDS+ASD compared to the conventional SNEDDS whilst containing 3 times less lipid than the latter. Furthermore, superSNEDDS+ASD were able to keep the drug solubilised during *in vitro* lipolysis to the same degree as the conventional SNEDDS. These findings suggest that dissolving an ASD in a superSNEDDS can contribute to the development of novel oral delivery systems with increased bioavailability for poorly water-soluble drugs.

1. Introduction

In the current drug discovery pipelines, an increasing number of potential conventional drug candidates display poor-water solubility [1]. The Biopharmaceutics Classification System (BCS) proposed by Amidon et al., classifies these drugs in class II (low solubility, high permeability) or class IV (low solubility, low permeability) [2]. Compounds belonging to these two classes, tend to have low absorption after oral administration, leading to low oral bioavailability. This presents a major challenge for drug development of poorly-water soluble drugs [3,4].

Orally administered drugs must dissolve in the gastrointestinal tract (GIT) fluids, in order to permeate the intestinal membrane and reach their target, to elicit the desired therapeutic response. BCS class II and IV compounds often need enabling drug delivery approaches in order to achieve a satisfactory absorption. The two most often applied enabling technologies are lipid based formulations, *e.g.* self-nanoemulsifying drug delivery systems (SNEDDS) and amorphous solid dispersions (ASD) [5].

* Corresponding author.
E-mail addresses: venkatasubramanian.ramakrishnan@sund.ku.dk (R. Venkatasubramanian), sophie.strindberg@sund.ku.dk (S. Strindberg), scheyla.siqueira@sund.ku.dk (S.D. Siqueira-Jørgensen), livia.pagano@uniroma1.it (L. Pagano), frank.romanski@basf.com (F.S. Romanski), nitin.swarnakar@basf.com (N.K. Swarnakar), thomas.rades@sund.ku.dk (T. Rades), anette.mullertz@sund.ku.dk (A. Müllertz).
[1] Authors contributed equally to this work.

https://doi.org/10.1016/j.jconrel.2022.06.057
Received 21 December 2021; Received in revised form 20 May 2022; Accepted 28 June 2022
Available online 8 July 2022

SNEDDS are isotropic mixtures of oils, surfactants and co-solvents, usually containing the drug dissolved in the lipid mixture. Upon gentle agitation in aqueous media (*e.g.* GIT fluids) the SNEDDS form nano-emulsion droplets, containing the drug in solution [6,7]. Thereby SNEDDS are bypassing the potentially absorption limiting dissolution step for poorly soluble drugs in the GIT, and improve drug absorption [8,9]. One of the limitations of the application of SNEDDS is that the drug dose in each capsule is limited by the solubility of the drug in the SNEDDS preconcentrate [10]. Additionally, in order to avoid drug precipitation in the SNEDDS preconcentrate during storage, or during dispersion of the SNEDDS preconcentrate, drugs are typically loaded below the equilibrium solubility (S_{eq}) in the SNEDDS preconcentrates (usually at 50 to 90% S_{eq}) [11]. This reduces the applicability and relevance of using SNEDDS for many drugs, as multiple capsules are needed to reach the desired dose [12]. In an effort to overcome this issue, the concept of supersaturated SNEDDS (superSNEDDS), in which the drug is loaded at a concentration higher than its S_{eq}, has been introduced [13]. SuperSNEDDS have displayed equivalent or better performance compared to conventional SNEDDS in many preclinical pharmacokinetic studies, while decreasing the number of units of dosage forms needed for each administration, compared to conventional SNEDDS [14–17].

Amorphous solid dispersions (ASD), consist of the poorly soluble drug molecularly dispersed in an amorphous carrier, usually a hydrophilic polymer [18]. The polymer in the ASD stabilizes the otherwise thermodynamically unstable solubilised or amorphous form of the drug upon storage [19,20]. Additionally, some polymers acts as a polymeric precipitation inhibitors (PPI) for the dissolved drug, maintaining a supersaturated state upon dissolution of the drug in the GIT by preventing precipitation; an effect popularly known as the "parachute effect" [21].

Intestinal supersaturation is an important enabler to improve the absorption of poorly water soluble drugs [22]. To stabilize the supersaturated state of a drug after dispersion, addition of a PPI to lipid-based drug delivery systems (such as SNEDDS) has been explored. Gao et al. observed a prolonged drug supersaturation upon dispersion and 5-fold higher oral bioavailability in rats, upon addition of HPMC (as PPI) in paclitaxel loaded SNEDDS [23]. Furthermore, multiple studies have investigated combining SNEDDS and PPIs, with all studies demonstrating supersaturated drug concentration (upon dispersion of SNEDDS) compared to PPI-free SNEDDS [24,25], albeit containing drug loads below the S_{eq} in the SNEDDS preconcentrate. Bannow et al. demonstrated the feasibility of using a PPI to stabilize drug against crystallization even upon loading above the S_{eq} in the SNEDDS preconcentrate (superSNEDDS). This enabled the addition of higher drug loads in SNEDDS preconcentrate. Additionally, superSNEDDS with PPI displayed improved physical stability upon storage and prolonged supersaturation levels after emulsification [26].

Against this background, the aim of the study was to explore the possibility of combining the advantages of superSNEDDS and ASD and thereby a) increase the load of dissolved drug in the SNEDDS preconcentrate; b) improve the physical stability of the drug in the SNEDDS preconcentrate upon storage; c) improve the absorption of ritonavir following oral administration in rats; d) keep the drug in solution upon emulsification and digestion in a 2-step *in vitro* lipolysis set-up. Polyvinylpyrrolidone-vinyl acetate copolymers (PVP-VA64) was used as a PPI and was dissolved in the superSNEDDS preconcentrate as the polymeric component of an ASD with ritonavir (superSNEDDS+ASD). The performance of superSNEDDS+ASD was compared to relevant controls (conventional SNEDDS (with drug load $< S_{eq}$), superSNEDDS with a physical mix (PM) of ritonavir and PVP-VA64 (superSNEDDS+PM) and an aqueous suspension of ritonavir), bioavailability of ritonavir following oral administration (pharmacokinetic (PK) study in rats) and on its ability to keep the ritonavir in solution following emulsification of the SNEDDS (2-step *in vitro* lipolysis set-up).

2. Materials

Kolliphor® RH 40 (polyoxyl 40 hydrogenated castor oil), Kollidon® VA64 (polyvinylpyrrolidone-vinyl acetate copolymers; PVP-VA64) and ritonavir were kindly provided by BASF (Ludwigshafen, Germany). Maisine® CC (glyceryl monolinoleate) was kindly donated by Gattefossé (Saint-Priest, France). Lipoid lyso-phospatidylcholine (LPC) (from soybean, containing 80.0% LPC) was kindly donated by Lipoid GmbH (Ludwigshafen, Germany). Ethylenediaminetetraacetic acid (EDTA) tripotassium salt dihydrate coated plasma tubes were obtained from Sarstedt (Nümbrecht, Germany). Soybean oil, porcine pancreatic lipase extract, tris (hydroxymethyl) aminomethane (Tris), maleic acid, bile extract (bovine) (B-3883), 4-(2-hydroxyethyl)-1-piperazineethanesulfonic acid (HEPES), pepsin and lipase (from *Rhizopus oryzae)* were obtained from Sigma-Aldrich (St Louis, MO, USA). Deionized water was obtained from an SG Ultraclear water system (SG Water GmbH, Barsbüttel, Germany). Ethanol (Ph. Eur. Grade) was purchased from VWR (Herlev, Denmark). All other reagents used were of analytical grade.

3. Methods

3.1. Preparation of formulations

The SNEDDS preconcentrate was prepared according to the composition shown in Table 1. First soybean oil and Maisine® CC were mixed. Subsequently, Kolliphor® RH 40 (heated to 60 °C) was added to this mixture and was homogenized by magnetic stirring at room temperature (RT) for 2 hours [27]. Upon cooling down to RT, ethanol was added as a co-solvent and the isotropic mixture was stirred for another 2 h at RT. SNEDDS with Kollidon® VA64 (Polymer SNEDDS) were prepared by adding Kollidon® VA64 (5% *w*/w), followed by overnight magnetic stirring at 37 °C (Note: at this step, no ritonavir was added to the system).

The S_{eq} of ritonavir in SNEDDS was determined by adding an excess of the drug to 1.0 g of SNEDDS preconcentrate. The suspension was left to end-over-end rotation for 48 h, at RT, followed by centrifugation (15 min at 17,004*g* at 25 °C). The clear supernatant obtained was then diluted with isopropanol. The resulting samples were quantified by HPLC-UV on an Ultimate 3000 HPLC with auto sampler from Thermo Scientific (Waltham, MA, USA), employing a calibration curve from 1 to 500 μg/mL. All experiments and measurements were performed in triplicates.

The conventional SNEDDS was prepared by weighing ritonavir into SNEDDS preconcentrate at 90% of the S_{eq} in a dust-free screw-top glass vial with a magnetic bar. The formulation was stirred at RT overnight. For the preparation of the superSNEDDS and polymer superSNEDDS, ritonavir was weighed and added to the SNEDDS preconcentrate ($S_{eq} >$ 100%), sonicated for one hour at 60 °C and then further heated at 60 °C for 3 h. The clear and solid-free superSNEDDS and polymer superSNEDDS were then left at 37 °C overnight followed by equilibration to RT on the next day [28].

The ASD of ritonavir and Kollidon® VA64 was prepared by ball milling. 40 mg of crystalline ritonavir and 960 mg Kollidon® VA64 were weighed and placed into a 25 mL milling jar containing two 1.2 cm stainless steel balls, and milled at a frequency of 30 Hz for a total of 3 h, with a 5 min break at 1.5 h to prevent overheating of the samples.

Table 1
Composition of SNEDDS.

Components	Ratio (w/w) %
Soybean oil	27.5
Maisine® CC	27.5
Kolliphor® RH 40	35
Ethanol	10

Absence of residual crystallinity in the ASD was confirmed by XRPD (Fig. S1) and polarized light microscopy (PLM, data not shown). A physical mix (PM) of ritonavir and Kollidon® VA64 was prepared by gentle mixing in a mortar and pestle containing the exact composition as in the ASD. The ASD or PM were then added to selected superSNEDDS (at 60 °C) and the mixtures were magnetically stirred in a 37 °C heating cabinet overnight to generate clear and solid-free superSNEDDS+ASD or superSNEDDS+PM, respectively.

The aqueous suspension of ritonavir (11.0 mg/mL) was prepared by mixing the drug with 0.5% (*w/v*) methyl cellulose solution containing 5% propylene glycol (as a wetting agent).

3.2. Stability assessment of superSNEDDS+ASD

The evaluation of the physical stability of superSNEDDS+ASD was performed in two steps. Firstly, the superSNEDDS+ASD were visually observed (clear or turbid) after storing at RT for one hour, and then observed using polarized light microscopy (PLM) with a Zeiss Axiolab microscope (Carl Zeiss, Göttingen, Germany) for presence or absence of crystalline ritonavir. Ritonavir suspension and superSNEDDS of ritonavir were used as controls. Multiple samples (at least $n = 3$) of each formulation were investigated. Each sample was scanned over the entire sample area at various magnifications. Images were captured using a DeltaPix digital camera and Deltapix software version 1.6 (Maloev, Denmark).

3.3. Pharmacokinetic study in rats

The animal study was performed under license no. 2016-15-0201-00892 and has been approved by the Animal Welfare Committee, appointed by the Danish Ministry of Justice. All animal procedures were carried out in compliance with EC Directive 86/609/EEC and with the Danish laws regulating experiments on animals. Male Sprague-Dawley rats (Janvier lab, Saint Berthevin, France) were kept in the animal care facility under an inverted light cycle, standard food and water *ad libitum* for 1 week before entering the study. Prior to the day of the experiments, the rats were fasted for 12 h and water was available *ad libitum*. On the day of the experiments the rats weighed 303 ± 11 g. The animals were divided in four groups of six rats, and subsequently randomly assigned to receive different formulations. The rats were given access to standard feed seven hours after dosing. Irrespective of the formulation, all rats were administered the same dose of 11 mg ritonavir by oral gavage. Approximately 5 min before dosing, all formulations, except for the conventional SNEDDS, were dispersed in deionized water (40% formulation/ 60% water *(w/v)*, 1 mL dosing volume). For ease of administration, the conventional SNEDDS (which contains almost 3-times the lipid load of the superSNEDDS+ASD) were dosed as a pre-concentrate, followed by an immediate administration of deionized water (at a ratio of 60% conventional SNEDDS/ 40% water *(w/v)*, 1 mL dosing volume). The aqueous suspension of ritonavir (11.0 mg/mL, 1 mL dosing volume) was prepared by mixing the drug with 0.5% (w/v) methyl cellulose solution containing 5% propylene glycol (as a wetting agent). Blood samples of 200 μL were collected by tail vein puncture into EDTA coated tubes. Blood samples were taken at 0, 0.25, 0.5, 0.75, 1, 1.5, 2, 3, 4, 7 and 23 h after dosing. Plasma was collected after centrifugation (10 min at 6708*g* at 4 °C) and stored at −20 °C until further analysis. The animals were euthanized immediately prior to the last blood sample at 23 h, which was collected from the heart.

Table 2
Composition of the simulated gastric medium, bile buffer and intestinal medium.

Components	Simulated gastric medium	Bile buffer	Simulated intestinal medium
Bile salts (mM)	1.3	69.7	24.1
Phospholipids (mM)	0.8	9.5	3.7
Sodium chloride (mM)	111.7	139.4	119.6
Hepes (mM)	–	50	17
HCl (mM)	4	–	–
Calcium chloride (mM)	–	4.2	1.4
pH	2.4	8.1	7.5
Enzyme activity	450 U/mL(pepsin) 50 U/mL (*Rh. lipase*)	–	179 USP/mL (pancreatin)

3.4. Two step in vitro rat lipolysis

A two-step dynamic *in vitro* rat lipolysis model simulating rat gastric and intestinal conditions was used to mimic the rat GIT conditions. The media were prepared as described by Christfort *et. al*, with adjustments as displayed in Table 2 [29]. The gastric medium and the bile buffer were prepared and stirred overnight in a heating cabinet at 37 °C. Initially, 18 mL of the gastric medium was placed in a thermostatic glass vessel at 37 °C. The desired weight of formulation to achieve a 25.7 mg of ritonavir was added, followed by addition of 2 mL of freshly prepared solutions of pepsin (1 mL) and lipase (1 mL) in gastric medium (as a proxy for lingual lipase, which is secreted from lingual serous gland from the rat tongue, a fungal source (*Rhizopus oryzae*) of lipase was used) with activity of 450 U/mL and 50 U/mL respectively [30]. At 30 min, the intestinal step (simulating rat intestinal conditions) was initiated by adding 5.0 mL of bile buffer (Table 2) to the vessel and taking a sample. Subsequently, 5.0 mL of pancreatic extract in bile buffer, prepared immediately before use, was added to achieve an enzymatic activity of 179 USP/mL [31]. To prepare the pancreatic lipase solution, an amount of pancreatin equivalent to the desired activity was weighed out in a falcon tube before addition to the intestinal medium. The mixture was vortexed for 30 s until homogeneous and subsequently centrifuged (7 min at 2952*g* at 21 °C). The resulting pancreatic lipase solution (supernatant) was kept on ice until use.

The pH was controlled for the gastric (pH 2.4) and the intestinal (pH 7.5) steps of the lipolysis using a pH-stat apparatus (Metrohm Titrando 842, Tiamo Version 1.3, Herisau, Switzerland) by titration with 0.4 M NaOH. Gastric samples were taken immediately after addition of pepsin and gastric lipase (0 min) and at 5, 15 and 30 min. Intestinal samples were taken at 31 min (immediately after addition of pancreatin), 45, 60 and 90 min (Fig. 3) after the addition of the bile buffer. For both steps, two types of samples were taken: a) a 50 μL sample that was immediately added to 450 μL of isopropanol and quantified for the total ritonavir (solubilised and unsolubilised) content (labelled as *total sample*) b) a 500 μL sample that was added to a tube containing 5 μL of 1 M 4-Bromophyenylboronic acid (4-BPBA) in methanol to inhibit lipase activity. The sample was then centrifuged (15 min at 17,004*g* at 25 °C) to generate an aqueous phase and a pellet, that were both quantified for ritonavir after appropriate dilution with isopropanol using RP-HPLC (labelled as *aqueous* and *pellet sample*). The ritonavir solubilised fraction was obtained from *Eq.(1)*.

$$\%solubilised\ fraction\ of\ ritonavir = \frac{Concentration\ of\ ritonavir\ in\ aqueous\ sample}{Concentration\ of\ ritonavir\ in\ total\ sample}\ \mathrm{X}\ 100 \quad (1)$$

All experiments were performed in triplicates.

3.5. Analysis of ritonavir from in vivo and in vitro studies using reversed phase- high performance liquid chromatography

Ritonavir containing samples were analyzed using a Dionex HPLC systems consisting of UltiMate 3000 Ultraviolet (UV) detector, UltiMate 3000 auto sampler, UltiMate 3000 pump from Thermo Scientific (Waltham, MA, USA). Separation of ritonavir was achieved by using a Kinetex C-18 column (4.60 × 250 mm, 5 μm; for *in vivo* plasma samples and 4.60 × 150 mm, 5 μm; for the *in vitro* lipolysis samples) (Phenomenex, Værløse, Denmark). The mobile phase consisted of water labelled as solvent A and acetonitrile labelled as solvent B. The flow rate was set at 0.8 mL/min. A linear gradient from 30% to 70% of solvent B over 8 min was used. Ritonavir was detected at 210 nm by the UV detector.

A calibration curve for the *in vivo* studies was prepared by spiking 30 μL blank plasma with appropriate volumes of ritonavir standard solution (1.2 mg/mL of ritonavir in acetonitrile) and diluted with acetonitrile to result in solutions ranging from 0.04 to 1.2 mg/mL. The mixtures were vortexed for 10 s and centrifuged (10 min at 10,062*g* at 25 °C) in a MicroCL 17 centrifuge (ThermoFisher Scientific, Waltham, MA, USA). The clear supernatant was transferred into HPLC vials. Plasma samples containing ritonavir were prepared by adding 25 μL of the harvested plasma from the PK study in 100 μL of acetonitrile. The mixture was then vortexed and centrifuged as described above and the supernatant was added to HPLC vials *(Limit of detection 57 ng/mL; Limit of quantification: 172 ng/mL)*.

3.6. Data analysis

Data analysis was carried out using Microsoft Excel 2013 (Microsoft Office, Redmond, WA, USA) and GraphPad Prism 7 (GraphPad Software, San Diego, CA, USA). All statistical analyses were performed using GraphPad Prism 7. Statistical differences between the groups were analyzed using one-way ANOVA *($p = 0.05$)* including Tukey's *post hoc* test.

Table 3
Composition and stability of SNEDDS with and without the addition of ASD or PM.

Formulation	Drug load (% of S_{eq} in SNEDDS)[x]	Drug load (mg/g)	Kollidon® VA64 (mg/g of SNEDDS)	Stability
Conventional SNEDDS 90%[§]	90%	8.4	none	> 2 month
superSNEDDS 200%[x]	200%	18.6	none	>2 month
superSNEDDS 250%[x]	250%	23.2	none	<48 h
Polymer superSNEDDS 275%[x]	275%	25.6	50.2	14 days
superSNEDDS 250%[x] + 25%[x] ASD[§]	275%	25.6	50.2	>1 month
superSNEDDS 250%[x] + 50%[x] ASD[a]	300%	27.9	90.7	<1 month
superSNEDDS 250%[x] + 25%[x] PM[*,§]	275%	25.6	50.2	<1 h

[x] % of S_{eq} of ritonavir in SNEDDS (S_{eq}: 9.3 ± 0.6 mg/g).
[a] 4% w/w ritonavir in Kollidon® VA64 as ASD.
[*] Added as ball milled polymer.
[§] These formulations were carried forward to the in vivo study, and named conventional SNEDDS, superSNEDDS + ASD and superSNEDDS + PM, respectively.

4. Results and discussion

4.1. Preparation and stability of ritonavir loaded superSNEDDS

The S_{eq} of ritonavir in the SNEDDS was determined to be 9.3 ± 0.6 mg/g. With the aim of increasing the ritonavir load in the SNEDDS, the ability of ritonavir to supersaturate in the SNEDDS preconcentrate was assessed (Table 3). A supersaturation degree of 200% of the S_{eq} resulted in a stable superSNEDDS for >2 months at RT. Similar to ritonavir, other poorly water soluble drugs, such as halofantrine and simvastatin have previously been demonstrated to form stable (> 2 months) superSNEDDS [13,32]. However, increasing the drug load of ritonavir to 250% of S_{eq}, resulted in drug precipitation within 48 h.

Kollidon® VA64 was chosen as the PPI, since it has the ability to dissolve in SNEDDS preconcentrate [26]. The superSNEDDS 250% was chosen as a starting point, because the drug precipitated within 48 h, and therefore improvement in the stability of the supersaturated state could be easily assessed. To further increase the drug load, and stabilize the supersaturated state of the drug in the superSNEDDS, an ASD (containing 4% *w/w* of ritonavir) was prepared using Kollidon® VA64 was dissolved in to the superSNEDDS 250% (superSNEDDS+ASD) (Table 3). The addition of 2.2 mg/g ritonavir (corresponding to 25% of the S_{eq} in the SNEDDS) as an ASD to the superSNEDDS 250% (superSNEDDS+ASD), resulted in a drug load of 25.6 mg/g (or 275% of the S_{eq} in the SNEDDS), displayed improved physical stability for more than one month.

Fig. 1 shows polarized light micrographs of crystalline ritonavir (a), superSNEDDS 250% (b) and superSNEDDS+ASD (c) one month after preparation. Crystals are clearly observed in superSNEDDS 250%, whereas there was no crystallization in the superSNEDDS+ASD (drug load 275% of S_{eq} in SNEDDS).

In contrast to the superSNEDDS+ASD, a PM with exactly the same amount of ritonavir and Kollidon® VA64 added to the superSNEDDS 250% (superSNEDDS+PM) resulted in precipitation of the drug from the superSNEDDS within one hour of storage at RT. Furthermore, polymer superSNEDDS (containing the same amount of Kollidon® VA64 as superSNEDDS+ASD) were prepared and ritonavir was added (at 275% of S_{eq} in SNEDDS; polymer superSNEDDS 275%). The polymer superSNEDDS 275% displayed improved physical stability compared to superSNEDDS 250% (48 h) and superSNEDDS+PM (1 h). However, ritonavir precipitated from polymer superSNEDDS 275% within 14 days of preparation (storage at RT). Thus, adding ritonavir and Kollidon® VA64 as an ASD to superSNEDDS resulted in superior stabilization of the supersaturated state, compared to adding ritonavir and Kollidon® VA64 as a PM or adding ritonavir to polymer superSNEDDS. A possible explanation for the instability of superSNEDDS+PM could be due to the presence crystalline seeds in PM when compared to the ASD in superSNEDDS. Previously, Bannow et al. used Kollidon® VA64 as a PPI in superSNEDDS with the model drug simvastatin. The authors showed that addition of 20% *w*/w Kollidon® VA64 in superSNEDDS was able to maintain simvastatin in a supersaturated state for >6 months, while simvastatin precipitated within 2 h in the superSNEDDS without Kollidon® VA64 [26]. These results are in agreement to the findings in the current study, where addition of Kollidon® VA64 to SNEDDS (polymer superSNEDDS 275%) is able to maintain ritonavir in the supersaturated state for a longer period than superSNEDDS without Kollidon® VA64 (superSNEDDS 250%). However, addition of ASD to the superSNEDDS (superSNEDDS+ASD) is able to achieve and maintain a similar supersaturated state for >1 month, indicating further improvement in stability of the supersaturated state. This might be due to the slow dissolution of the ASD into the superSNEDDS 250%, leading to a "gentle" technique to supersaturate SNEDDS even further, as compared to dissolution of a large dose of crystalline drug in polymer superSNEDDS 275%.

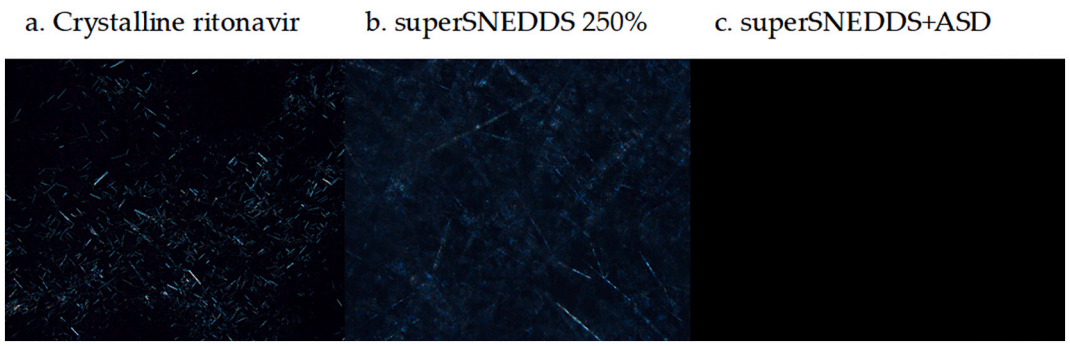

Fig. 1. Representative PLM images of a. crystalline ritonavir; b. superSNEDDS 250% (at 250% of ritonavir S_{eq} in SNEDDS; 48 h after preparation; and c. superSNEDDS+ASD (observation made after 1 month of storage at RT, no crystals were detetcted).

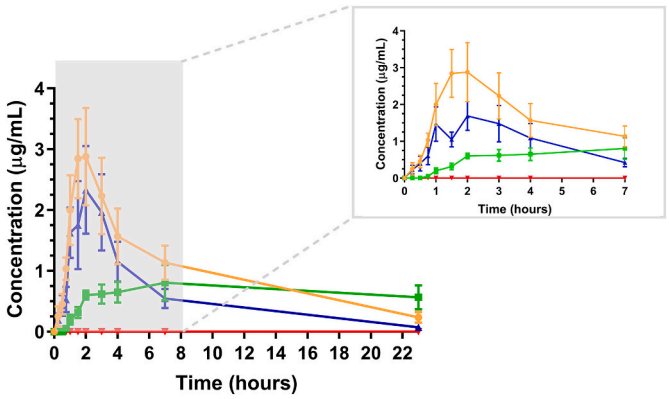

Fig. 2. Plasma concentration (µg/mL)-time (hours) profiles of ritonavir after oral administration of a. superSNEDDS+ASD (orange), b. conventional SNEDDS (green), c. superSNEDDS+PM (blue) and d. aqueous suspension (red) to rats. All data points are presented as mean ± SEM; n = 5–6. (For interpretation of the references to colour in this figure legend, the reader is referred to the web version of this article.)

Table 4
Pharmacokinetic (PK) parameters for ritonavir after oral administration to fasted rats. Data presented as mean ± SEM (n = 5–6).

Formulation	superSNEDDS + ASD	Conventional SNEDDS	superSNEDDS + PM	Aqueous suspension
C_{max} (µg/mL)	3.2 ± 0.6^{a}	1.0 ± 0.2^{b}	1.9 ± 0.3	Not detected
T_{max} (h)	1.7 ± 0.2^{c}	4.5 ± 1.3^{d}	1.5 ± 0.2	Not detected
$AUC_{0\text{-}7h}$ (µg.h.mL^{-1})	11.8 ± 5.7^{e}	3.9 ± 1.7^{f}	7.2 ± 4.0^{g}	Not detected
$AUC_{0\text{-}23h}$ (µg.h.mL^{-1})	22.8 ± 5.8^{h}	14.8 ± 5.7^{i}	11.0 ± 2.9^{k}	Not detected

Values with "a" are significantly different from numbers with "b" *($p < 0.05$)*. Values with "c" are significantly different from numbers with "d" *($p < 0.05$)*. Values with "e" are significantly different from numbers with "f" and "g" *($p < 0.05$)*. Values with "h" are significantly different from numbers with "i" and "k" *($p < 0.05$)*.

4.2. Pharmacokinetic study in rats

To evaluate if the superSNEDDS+ASD is able to influence ritonavir absorption, compared to the conventional SNEDDS and the superSNEDDS+PM, a PK study in rats was carried out. An aqueous suspension of ritonavir was included as control. One rat each from the conventional SNEDDS and aqueous suspension group were excluded due to incorrect dosing. Furthermore, the PK-profile of one rat from the superSNEDDS+ASD group was multiple times higher than the average profile, and therefore was considered an outlier and excluded from the current study.

Fig. 2 displays the mean plasma concentration-time profiles for ritonavir. The maximum plasma concentration (C_{max}), time to reach C_{max} (T_{max}), $AUC_{0\text{-}2h}$, $AUC_{0\text{-}7h}$ and $AUC_{0\text{-}23h}$ are provided in Table 4.

The aqueous suspension did not result in any detectable plasma levels of ritonavir.

Oral dosing of ritonavir in the superSNEDDS+ASD resulted in a statistically higher C_{max}*($p = 0.006$)*, earlier T_{max}*($p = 0.019$)* and higher $AUC_{0\text{-}23h}$*($p = 0.028$)* compared to the conventional SNEDDS. The late T_{max} obtained from the conventional SNEDDS could be due to the high amount of lipids administered with the conventional SNEDDS, possibly resulting in a delay in gastric emptying, as compared to superSNEDDS+ASD and superSNEDDS+PM. This is represented by the "lag phase" seen in Fig. 2; ritonavir was not detected in the plasma samples until 1 h after dosing of the conventional SNEDDS. In addition, the $AUC_{0\text{-}7h}$ is significantly higher for the superSNEDDS+ASD compared to the conventional SNEDDS (3-fold increase, $p = 0.014$) (Fig. 2), indicating that superSNEDDS+ASD is able to generate a higher concentration of ritonavir available at the site of absorption when compared to the conventional SNEDDS.

Comparing superSNEDDS+ASD with superSNEDDS+PM, no statistical difference was found for C_{max}*($p = 0.123$)* and T_{max}*($p = 0.152$)*. However, $AUC_{0\text{-}7h}$ and $AUC_{0\text{-}23h}$ were significantly higher for the superSNEDDS+ASD compared to the superSNEDDS+PM (1.6-fold increase, $p = 0.035$ and 2.1-fold increase, $p = 0.030$, respectively). This indicates that the absorption of ritonavir is higher and is continuing for a longer time for the superSNEDDS+ASD than for superSNEDDS+PM, possibly due to precipitation of ritonavir in the GIT following dosing of

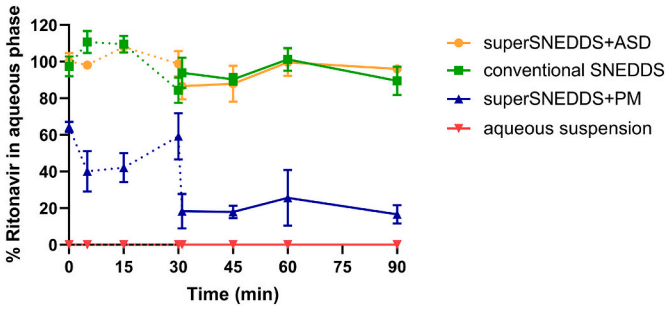

Fig. 3. Solubilization and digestion of ritonavir in a. superSNEDDS+ASD (orange), b. conventional SNEDDS (green), c. superSNEDDS+PM (blue) and d. aqueous suspension (red) in the 2-step *in vitro* lipolysis mimicking the gastrointestinal tract of a rat. Dashed and filled lines represent gastric and intestinal phase, respectively. (Mean ± SD; n = 3). (For interpretation of the references to colour in this figure legend, the reader is referred to the web version of this article.)

superSNEDDS+PM.

4.3. Two-step in vitro rat lipolysis

To evaluate if the PK data described above could be simulated *in vitro*, and explain some of the differences observed, a study was carried with the four formulations in a two-step *in vitro* lipolysis simulating rat gastric and intestinal conditions.

The amount of ritonavir dosed in the lipolysis media was kept constant at 25.7 mg for all the formulations. Fig. 3 shows the amount of solubilised ritonavir in the aqueous phase, relative to the total ritonavir content (solubilised and precipitated) as a function of time. No ritonavir was detected in the aqueous phase from the aqueous suspension, indicating the solubilizing capacity of superSNEDDS+ASD, conventional SNEDDS and superSNEDDS+PM for presenting ritonavir in the aqueous phase.

The digestion of all three SNEDDS (conventional SNEDDS, superSNEDDS+ASD and superSNEDDS+PM) generates free fatty acids and mono- and di-glycerides, which are solubilised in mixed micelles formed by the bile salts and phospholipids in the media. These mixed micellar systems possess high solubilizing capacity that often are able to keep poorly soluble drugs solubilised [7,33,34].

At time zero, before the addition of pepsin and gastric lipase, the complete dose of ritonavir was recovered in the aqueous phase for both the superSNEDDS+ASD and conventional SNEDDS. This trend continued into the intestinal phase, where 100% of the initial dose of ritonavir was recovered in the aqueous phase for both SNEDDS. Although superSNEDDS+ASD contains 3-fold less lipid than the conventional SNEDDS, at the same dose of ritonavir, superSNEDDS+ASD were able to keep the dose of ritonavir solubilised to the same degree as the conventional SNEDDS.

For the superSNEDDS+PM, only 64 ± 4% of the ritonavir dose was solubilised in the aqueous phase at time zero, significantly less than the amount of ritonavir solubilised at time zero for the superSNEDDS+ASD *($p = 0.0001$)*. This indicates the advantage of adding an ASD of ritonavir to the superSNEDDS instead of a PM as 100% of the initial dose was recovered in the aqueous phase for the superSNEDDS+ASD.

The $AUC_{0\text{-}23h}$ obtained from the *in vivo* PK-study ($AUC_{0\text{-}23h}$) displayed a good rank order correlation with the % ritonavir in the aqueous phase from the *in vitro* lipolysis study for all four formulation, in the order: superSNEDDS+ASD ≥ conventional SNEDDS > superSNEDDS+PM > aqueous suspension. However, the two-step *in vitro* lipolysis model does not capture the reduced C_{max} of the conventional SNEDDS compared to superSNEDDS+ASD. This can be attributed to the lack of simulation of the gastric emptying in the *in vitro* lipolysis model. As described above, the high lipid load can reduce the gastric emptying *in vivo*, thereby being responsible for increasing T_{max} and lowering C_{max}. The used two-step *in vitro* lipolysis model only observes the solubilised state of the drug, which is assumed to be available for absorption. In order to improve the predictability of the *in vitro* models, some changes to the model can be considered, such as implementing a calorie based gastric emptying [35], or including an absorption step [36–38]. These changes could possibly improve the predictability of the current two-step *in vitro* lipolysis model.

5. Conclusion

In this study, we combined preformed superSNEDDS (250%) with an ASD and achieved a maximized degree of supersaturation (275%; stabilized by the polymer from the ASD) due to the gentle process of dissolving more amorphous drug (also from the ASD) in the superSNEDDS. Hereby it was possible not only to achieve a higher drug load but also an increased physical stability (>1 month) compared to superSNEDDS 250%, from which the poorly water soluble model drug ritonavir recrystallised in <48 h. In the superSNEDDS+PM, where the amorphous drug and polymer were added separately, ritonavir precipitated within one hour. The *in vivo* PK study in rats demonstrated that absorption of ritonavir following oral gavage was higher for the superSNEDDS+ASD compared to both the conventional SNEDDS ($AUC_{0\text{-}7h}$ and C_{max}) and the superSNEDDS+PM ($AUC_{0\text{-}23h}$). Further, the superSNEDDS+ASD were able to keep the drug solubilised during the two-step *in vitro* lipolysis (simulating the rat gastric and intestinal GI tract conditions) to the same degree as the conventional SNEDDS, while containing less lipid. The superSNEDDS+PM was not able to keep ritonavir solubilised to the same degree as superSNEDDS+ASD in the *in vitro* lipolysis, indicating a strong physico-chemical difference within the systems. Further studies are needed to understand these mechanisms. The ritonavir content in aqueous phase from the two-step *in vitro* lipolysis was able to predict the $AUC_{0\text{-}23h}$ rank order, as observed in the *in vivo* PK study. However, the *in vitro* model could not capture the slow gastric emptying of conventional SNEDDS, which could have occurred *in vivo*. The present study provides a novel formulation strategy to enable higher drug loads and improve the absorption of a poorly-water soluble drug, namely to combine lipid drug delivery systems with amorphous drug in polymer.

CRediT authorship contribution statement

Georgia-Ioanna Nora: Investigation, Methodology, Writing – original draft, Formal analysis, Visualization. **Ramakrishnan Venkatasubramanian:** Investigation, Methodology, Writing – original draft, Formal analysis, Visualization. **Sophie Strindberg:** Methodology, Writing – review & editing. **Scheyla Daniela Siqueira Jørgensen:** Methodology, Writing – review & editing. **Livia Pagano:** Methodology, Writing – review & editing. **Francis S. Romanski:** Resources, Writing – review & editing. **Nitin K. Swarnakar:** Resources, Writing – review & editing. **Thomas Rades:** Conceptualization, Methodology, Project administration, Resources, Writing – review & editing, Supervision, Data curation. **Anette Müllertz:** Conceptualization, Methodology, Project administration, Resources, Writing – review & editing, Supervision, Data curation.

Declaration of Competing Interest

The authors declare that they have no competing financial interests or personal relationships that could have appeared to have influenced the work in this manuscript.

Appendix A. Supplementary data

Supplementary data to this article can be found online at https://doi.org/10.1016/j.jconrel.2022.06.057.

References

[1] S.V. Jermain, C. Brough, R.O. Williams, Amorphous solid dispersions and nanocrystal technologies for poorly water-soluble drug delivery – an update, Int. J. Pharm. 535 (2018) 379–392.
[2] G.L. Amidon, H. Lennernäs, V.P. Shah, J.R. Crison, A theoretical basis for a biopharmaceutic drug classification: the correlation of in vitro drug product dissolution and in vivo bioavailability, Pharm. Res. 12 (1995) 413–420.
[3] Amorphous Solid Dispersions, Theory and Practice, Springer, 2014, https://doi.org/10.1007/978-1-4939-1598-9_23.
[4] H.D. Williams, et al., Toward the establishment of standardized invitro tests for lipid-based formulations, Part 1: Method parameterization and comparison of invitro digestion profiles across a range of representative formulations, J. Pharm. Sci. 798–809 (2012), https://doi.org/10.1002/jps.
[5] J. Siepmann, et al., Lipids and polymers in pharmaceutical technology: lifelong companions, Int. J. Pharm. 558 (2019) 128–142.
[6] C.W. Pouton, Formulation of poorly water-soluble drugs for oral administration: physicochemical and physiological issues and the lipid formulation classification system, Eur. J. Pharm. Sci. 29 (2006) 278–287.
[7] A. Mllertz, A. Ogbonna, S. Ren, T. Rades, New perspectives on lipid and surfactant based drug delivery systems for oral delivery of poorly soluble drugs, J. Pharm. Pharmacol. 62 (2010) 1622–1636.
[8] C.J.H. Porter, N.L. Trevaskis, W.N. Charman, Lipids and lipid-based formulations: optimizing the oral delivery of lipophilic drugs, Nat. Rev. Drug Discov. 6 (2007) 231–248.

[9] D.G. Fatouros, A. Mullertz, In vitro lipid digestion models in design of drug delivery systems for enhancing oral bioavailability, Expert Opin. Drug Metab. Toxicol. 4 (2008) 65–76.
[10] T. Do Thi, et al., Formulate-ability of ten compounds with different physicochemical profiles in SMEDDS, Eur. J. Pharm. Sci. 38 (2009) 479–488.
[11] N. Thomas, R. Holm, A. Müllertz, T. Rades, In vitro and in vivo performance of novel supersaturated self-nanoemulsifying drug delivery systems (super-SNEDDS), J. Control. Release 160 (2012) 25–32.
[12] N. Thomas, R. Holm, T. Rades, A. Müllertz, Characterising lipid lipolysis and its implication in lipid-based formulation development, AAPS J. 14 (2012) 860–871.
[13] N. Thomas, et al., Supersaturated self-nanoemulsifying drug delivery systems (super-SNEDDS) enhance the bioavailability of the poorly water-soluble drug simvastatin in dogs, AAPS J. 15 (2013) 219–227.
[14] N. Thomas, et al., Supersaturated self-nanoemulsifying drug delivery systems (super-SNEDDS) enhance the bioavailability of the poorly water-soluble drug simvastatin in dogs, AAPS J. 15 (2013) 219–227.
[15] N. Thomas, et al., In vitro lipolysis data does not adequately predict the in vivo performance of lipid-based drug delivery systems containing fenofibrate, AAPS J. 16 (2014) 539–549.
[16] S.D.V.S. Siqueira, et al., Influence of drug load and physical form of cinnarizine in new SNEDDS dosing regimens: in vivo and in vitro evaluations, AAPS J. 19 (2017) 587–594.
[17] M.M. Knopp, et al., Effect of polymer type and drug dose on the in vitro and in vivo behavior of amorphous solid dispersions, Eur. J. Pharm. Biopharm. 105 (2016) 106–114.
[18] S. Baghel, H. Cathcart, N.J. O'Reilly, Polymeric amorphous solid dispersions: a review of Amorphization, crystallization, stabilization, solid-state characterization, and aqueous Solubilization of biopharmaceutical classification system class II drugs, J. Pharm. Sci. 105 (2016) 2527–2544.
[19] B.C. Hancock, M. Parks, What is the true solubility advantage for amorphous pharmaceuticals, Pharm. Res. 17 (2000) 397–404.
[20] M.M. Knopp, et al., Effect of polymer type and drug dose on the in vitro and in vivo behavior of amorphous solid dispersions, Eur. J. Pharm. Biopharm. 105 (2016) 106–114.
[21] P. Augustijns, M.E. Brewster, Supersaturating drug delivery systems: fast is not necessarily good enough, J. Pharm. Sci. 101 (2012) 7–9.
[22] R. Takano, et al., Quantitative analysis of the effect of supersaturation on in vivo drug absorption, Mol. Pharm. 7 (2010) 1431–1440.
[23] P. Gao, et al., Development of a supersaturable SEDDS (S-SEDDS) formulation of paclitaxel with improved oral bioavailability, J. Pharm. Sci. 92 (2003) 2386–2398.
[24] E.J.A. Suys, D.K. Chalmers, C.W. Pouton, C.J.H. Porter, Polymeric precipitation inhibitors promote Fenofibrate supersaturation and enhance drug absorption from a type IV lipid-based formulation, Mol. Pharm. 15 (2018) 2355–2371.
[25] P. Gao, et al., Enhanced Oral bioavailability of a poorly water soluble drug PNU-91325 by Supersaturatable formulations, Drug Dev. Ind. Pharm. 30 (2004) 221–229.
[26] J. Bannow, Y. Yorulmaz, K. Löbmann, A. Müllertz, T. Rades, Improving the drug load and in vitro performance of supersaturated self-nanoemulsifying drug delivery systems (super-SNEDDS) using polymeric precipitation inhibitors, Int. J. Pharm. 575 (2020) 118960.
[27] S.D. Siqueira Jørgensen, T. Rades, H. Mu, K. Graeser, A. Müllertz, Exploring the utility of the chasing principle: influence of drug-free SNEDDS composition on solubilization of carvedilol, cinnarizine and R3040 in aqueous suspension, Acta Pharm. Sin. B 9 (2019) 194–201.
[28] S.D. Siqueira Jørgensen, et al., The ability of two in vitro lipolysis models reflecting the human and rat gastro-intestinal conditions to predict the in vivo performance of SNEDDS dosing regimens, Eur. J. Pharm. Biopharm. 124 (2018) 116–124.
[29] J.F. Christfort, et al., Developing a predictive in vitro dissolution model based on gastrointestinal fluid characterisation in rats, Eur. J. Pharm. Biopharm. 142 (2019) 307–314.
[30] T. Tran, et al., Using in vitro lipolysis and SPECT/CT in vivo imaging to understand oral absorption of fenofibrate from lipid-based drug delivery systems, J. Control. Release 317 (2020) 375–384.
[31] P.C. Christophersen, et al., Fed and fasted state gastro-intestinal in vitro lipolysis: in vitro in vivo relations of a conventional tablet, a SNEDDS and a solidified SNEDDS, Eur. J. Pharm. Sci. 57 (2014) 232–239.
[32] N. Thomas, R. Holm, A. Müllertz, T. Rades, In vitro and in vivo performance of novel supersaturated self-nanoemulsifying drug delivery systems (super-SNEDDS), J. Control. Release 160 (2012) 25–32.
[33] A.T. Larsen, et al., Bioavailability of cinnarizine in dogs: effect of SNEDDS loading level and correlation with cinnarizine solubilization during in vitro lipolysis, Pharm. Res. 30 (2013) 3101–3113.
[34] C.J.H. Porter, et al., Use of in vitro lipid digestion data to explain the in vivo performance of triglyceride-based Oral lipid formulations of poorly water-soluble drugs: studies with Halofantrine, J. Pharm. Sci. 93 (2004) 1110–1121.
[35] S.D. Siqueira Jørgensen, et al., The ability of two in vitro lipolysis models reflecting the human and rat gastro-intestinal conditions to predict the in vivo performance of SNEDDS dosing regimens, Eur. J. Pharm. Biopharm. 124 (2018) 116–124.
[36] M. Klitgaard, A. Müllertz, R. Berthelsen, Estimating the Oral Absorption from Self-Nanoemulsifying Drug Delivery Systems Using an In Vitro Lipolysis-Permeation Method, 2021, pp. 1–14.
[37] J. Keemink, E. Mårtensson, C.A.S. Bergström, Lipolysis-permeation setup for simultaneous study of digestion and absorption in vitro, Mol. Pharm. 16 (2019) 921–930.
[38] L.C. Alskär, et al., Effect of lipids on absorption of carvedilol in dogs: is coadministration of lipids as efficient as a lipid-based formulation? J. Control. Release 304 (2019) 90–100.